**OPEN**

# Hydrogen sulfide and resolution of acute inflammation: A comparative study utilizing a novel fluorescent probe

Neil Dufton, Jane Natividad, Elena F. Verdu & John L. Wallace

Farncombe Family Digestive Health Research Institute, McMaster University, Hamilton, Ontario, Canada.

**Hydrogen sulfide is an essential gasotransmitter associated with numerous pathologies. We assert that hydrogen sulfide plays an important role in regulating macrophage function in response to subsequent inflammatory stimuli, promoting clearance of leukocyte infiltrate and reducing TNF-α levels *in vivo* following zymosan-challenge. We describe two distinct methods of measuring leukocyte hydrogen sulfide synthesis; methylene blue formation following zinc acetate capture and a novel fluorescent sulfidefluor probe. Comparison of these methods, using pharmacological tools, revealed they were complimentary *in vitro* and *in vivo*. We demonstrate the application of sulfidefluor probe to spectrofluorimetry, flow cytometry and whole animal imaging, to monitor the regulation of hydrogen sulfide synthesis *in vivo* during dynamic inflammatory processes. Both methodologies revealed that granulocyte infiltration negatively affects hydrogen sulfide synthesis. Our report offers an insight into the profile of hydrogen sulfide synthesis during inflammation and highlight opportunities raised by the development of novel fluorescent hydrogen sulfide probes.**

Hydrogen sulfide ($H_2S$), which is a gasotransmitter such as nitric oxide and carbon monoxide, is implicated in a variety of inflammatory[1] and vascular disorders[2], associated with both pro- and anti-inflammatory signaling[3]. We have previously demonstrated numerous anti-inflammatory effects of $H_2S$ donors: reducing adhesion and rolling of circulating leukocytes in inflamed microvasculature[4], accelerated resolution of experimental colitis[5] and enhanced gastric ulcer healing[6]. The capacity of tissues, such as the brain, liver and colon, to synthesize $H_2S$ is well-documented[7]. Furthermore, $H_2S$ synthesis is elevated in various inflammatory conditions[5]. However, the contribution and effect of endogenous $H_2S$ on infiltrating leukocytes in inflammatory models has not been well characterized.

Primarily studies have focused on the effects of exogenous sources of $H_2S$, utilizing compounds such as sodium hydrosulfide (NaHS) in immortalized cell lines. Despite a large study base the application of this ubiquitous $H_2S$-donor is often disputed because of the kinetics of $H_2S$ release and the concentrations used. A comparative study showing differences between fast- (NaHS) and slow-release (GYY4137) $H_2S$ donors showed an increase in inflammatory markers with high concentrations of NaHS compared to inhibitory effects of GYY4137[8]. It has since been reported that high concentrations ($\sim$1 mM) of NaHS trigger TNF-α and IL-1 release from IFN-γ-primed U937 cells in a NFκB-dependent fashion[9]. Furthermore, a study utilizing primary macrophages (Mφ) revealed LPS-induced up-regulation of a $H_2S$ synthesizing enzyme, CSE, in a concentration-dependent manner[10]. Conversely, $H_2S$ donors have been reported to reduce LPS-induced TNF-α release by microglia[11,12] and NFκB activation in RAW 264.7 macrophages[13].

A second approach has been to inhibit endogenous $H_2S$ synthesis that occurs via the 'classical' pathway, through two cystathionine enzymes, cystathionine-β-synthase (CBS) and cystathionine γ-lyase (CSE). It is notable that transgenic mice deficient for CBS suffer severe growth retardation and mortality within 5 weeks of birth[14]. CSE deficiency leads to a milder phenotype with mice displaying age-related hypertension and sex-related hyperhomocysteinemia[15]. These enzymes have also been targeted with a variety of pharmacological tools, with O-(carboxymethyl) hydroxylamine hemihydrochloride (CHH) and L-propargylglycine (L-PAG) predominantly used to inhibit CBS and CSE, respectively. However, as with the $H_2S$ donors, their actions have been described as both pro-[16] and anti-inflammatory[17,18]. Furthermore, recent studies have begun to characterize 'alternative' pathways of $H_2S$ production[19], with few specific pharmacological tools available to assess their physiological impact.

The interpretation of studies reported above might not only hinge on the pharmacological tools used but also on how each laboratory measures H₂S in biological samples. Many accurate methods have been described including chromatography[20], polarographic electrodes[21] and lead acetate capture on filter paper. The later remains a gold standard for quantifying bacterial H₂S production[22]. We have utilized a variation of the lead acetate technique, optimized for tissue synthesis of H₂S by methylene blue formation[5]. During 2011 a series of papers revealed new advances in applying highly selective fluorescence probes to measure H₂S in living cells[23–25]. We have combined the two techniques to investigate the regulation of leukocyte H₂S synthesis. In this comparative study we characterized the profile of H₂S synthesis in vitro and in vivo in the context of inflammation using traditional laboratory assays along side state-of-the-art imaging techniques to assess H₂S synthesis in vivo in real-time.

## Results

**Primary macrophage H₂S production is partially dependent on cystathionine enzymes.** To determine if human peripheral blood mononuclear cells (PBMC)-derived MΦ had the enzymatic machinery to synthesize H₂S we assessed the expression of two cysthationine enzymes, CBS and CSE, by immunohistochemistry (Fig. 1 B and C respectively). PBMC-derived MΦ were incubated overnight with either mouse anti-human CBS or CSE antibodies (1:250), or IgG isotype control (Fig. 1 A). The SF5 probe was used to visualize intracellular H₂S in primary murine P-Gel-derived MΦ compared to vehicle alone (Fig. 1 D and E respectively).

A comparison of methylene blue formation versus fluorescent intensity of the SF5 probe was investigated by a concentration response study using NaHS as the source of H₂S (Fig. 1 F). Methylene blue (open squares) had ~100-fold greater sensitivity for measuring H₂S in this cell-free assay than SF5 (closed circles).

To assess H₂S synthesis in primary murine cells we used P-Gel-derived MΦ. H₂S sulfide synthesis from MΦ lysates was primarily evaluated by methylene blue formation using a zinc acetate capture method. Lysates were incubated in the presence or absence of the co-factors, L-cysteine and P5P, as well as the cystathionine inhibitors, L-PAG and CHH (Fig. 1G). H₂S synthesis was dependent on the presence of both L-cysteine and P5P, with a significant ($P<0.01$), concentration-dependent reduction with inhibition of the cysthationine enzymes (Fig. 1I). The SF5 probe was visible in living cell preparations (Fig. 1E) and therefore was assessed by measuring fluorescence intensity following the addition of SF5 probe (1 μM) to P-Gel-derived MΦ in a 24-well plate (Fig. 1H–J). Fluorescence was assessed every 2 min for 1 h and area-under-the-curve (AUC) was calculated for each treatment. Addition of L-cysteine and P5P to the culture medium for 1 h had no effect on intracellular H₂S formation (Fig. 1 H). Inhibition of the cystathionine enzymes, using L-PAG and CHH, significantly reduced ($P<0.05$) H₂S synthesis in a concentration-dependent manner utilizing both analytical approaches (Fig. 1I and J).

**Hydrogen sulfide primes macrophage responses to LPS stimulation.** We investigated the effect of NaHS and LPS, alone or in combination, on synthesis of H₂S, measured either by methylene blue formation or SF5 fluorescence (Fig. 2A and B respectively). Both methods detected a significant reduction ($P<0.05$) in H₂S synthesis following 4 h LPS stimulation. Pretreatment with NaHS (30 μM; −15 min) prevented the inhibition of H₂S synthesis by LPS (Fig. 2A and B). Furthermore, cysthationine activity was shown to be enhanced ($P<0.05$) by the pre-treatment with NaHS (Fig. 2A).

The effects of H₂S on several markers of MΦ function (TNF-α, IL-10, cAMP and arginase-1) were also examined. We observed that 4 h treatment with NaHS alone (30 or 100 μM) had no significant effect on the synthesis of H₂S, TNF-α or IL-10 release, or on intracellular cAMP levels and arginase activity (Fig. 2A–F). In contrast, 15 min pre-incubation with NaHS prior to LPS stimulation (4 h) significantly affected each of these markers ($P<0.05$), with the exception of IL-10 (Fig. 2D). TNF-α release was reduced ($P<0.05$) by pre-treatment with 100 μM NaHS compared to LPS alone (Fig. 2A). Levels of intracellular cAMP and arginase activity were significantly increased when the MΦ were exposed to 30 μM NaHS prior to LPS (Fig. 2C and D respectively), as compared to the control group.

To assess whether NaHS produced its effects by regulating intracellular signaling we investigated phosphorylation of Akt and IκB-α expression using western blotting (Fig. 3A and B). NaHS (100 μM) alone was shown to induce both phosphorylation of Akt and IκB-α expression over a period of 60 min (Fig. 3A). LPS stimulation (300 ng/ml; 30min) also induced phosphorylation of Akt, which was inhibited by pre-treatment with NaHS across the concentration range (Fig. 3B).

The ability of NaHS to regulate functional behaviour of MΦ was evaluated by bacterial phagocytosis and fMLP-induced chemotaxis (Fig. 3C and D respectively). Bacterial ingestion of ampicillin-resistant E.coli was significantly ($P<0.01$) increased in P-Gel-derived MΦ pre-treated with NaHS (Fig. 3C). The addition of LPS also increased bacterial ingestion ($P<0.001$). Furthermore, pre-treatment of P-Gel-derived MΦ with 100 μM NaHS, prior to LPS, significantly ($P<0.001$) reduced viability of bacteria by MTT growth assay (Fig. 3C). NaHS alone had no significant effect on the chemotactic function of bone marrow-derived MΦ (Fig. 3D). The mobilization of MΦ towards fMLP (10 μM) was significantly ($P<0.05$) enhanced by NaHS in a concentration-dependent manner (Fig. 3D).

**Characterization of hydrogen sulfide synthesis during acute and resolving inflammation.** We used two models of acute inflammation: zymosan-induced peritonitis (Fig. 4) and zymosan-induced air pouch (Fig. 5), to characterize H₂S synthesis by tissue and infiltrating leukocytes during a 48 h time course.

H₂S synthesis by resident and infiltrating leukocytes was measured by either methylene blue formation (Fig. 4A) or SF5 fluorescence (Fig. 4B-H). For methylene blue formation infiltrating leukocytes were harvested from the peritoneum at a given time point, lysed, then incubated with L-cysteine and P5P (open bars; right Y-axis) and normalized to cell number. Total cell numbers infiltrating the peritoneum are overlaid (black squares) (Fig. 4A). H₂S synthesis mirrored the peak leukocyte infiltration, reflected in a significant ($P<0.001$) reduction at 4 h. H₂S synthesis by infiltrating leukocytes increased as inflammation resolved (48 h). A second set of experiments was performed in which the SF5 probe was injected into the peritoneum 30 min before each sample collection. Fluorescence intensity of the cell exudates was measured by spectrofluorometry (Fig. 4B) or by flow cytometry (Fig. 4C–H). The fluorescence profile of the exudates was broadly consistent with the data obtained by methylene blue formation, with minimal SF5 fluorescence at the time of peak cell infiltration (24 h). To further investigate the leukocyte-H₂S profile we applied flow cytometry with the addition of neutrophils (Gr-1ʰⁱ) or monocyte/macrophage (F4/80) markers. The histograms and bar graphs are representative of total infiltrating leukocytes (Fig. 4C and F), Gr-1ʰⁱᵍʰ (Fig. 4D and G) and F4/80⁺ (Fig. 4E and H). Each time point is represented by a different colour; 0 h orange, 4 h blue, 24 h green and 48 h red with black denoting the isotype control (Fig. 4C–E). There was a significant ($P<0.01$) reduction in the total leukocyte median fluorescence intensity (MFI) at 4 h, which recovered to basal levels at 24 and 48 h (Fig. 4F). Although the neutrophil (Gr-1ʰⁱ) profile shows no significance between groups (Fig. 4G), it is important to note the differing characteristics of each time point on the histograms. Very few granulocytes were present at 0 h, followed by a sharp peak at 4 h which becomes more diffuse by 24/48 h (Fig. 4D). Conversely, F4/80⁺ cells significantly ($P<0.05$) increased in fluorescence at 24 and 48 h (Fig. 4H). The characteristics of the leukocyte infiltrate at each time
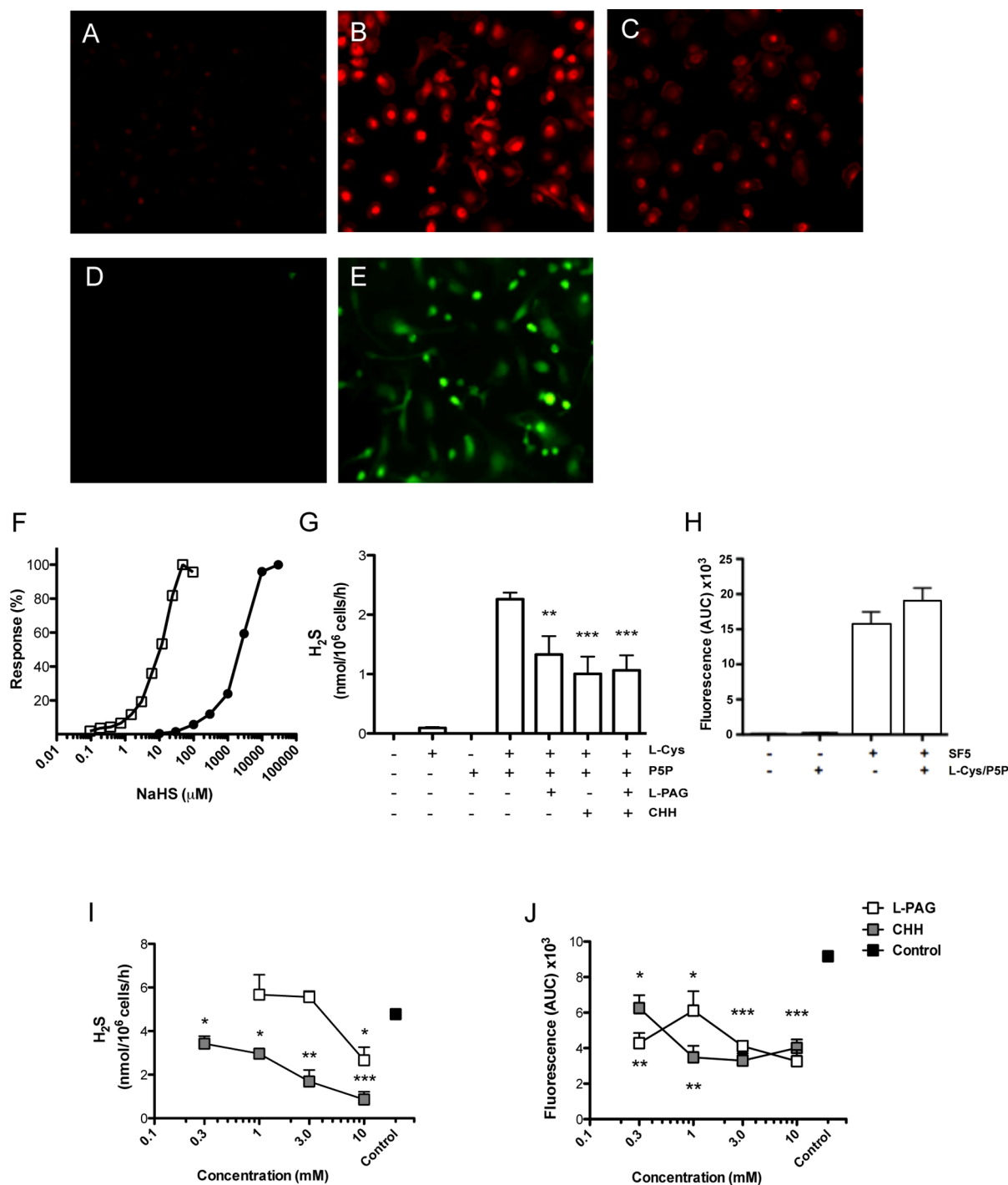
**Figure 1 | Hydrogen sulfide synthesis by primary macrophages is partially dependent on classical cystathionine enzymes.** Immunohistochemical analysis of human PBMC-derived MΦ incubated with (A) mouse IgG2 Isotype, (B) mouse anti-human CBS, and (C) mouse anti-human CSE (Abnova). Data are representative images of samples from three healthy male donors. Murine P-Gel-derived MΦ were incubated for 30 min with either (D) vehicle or (E) 1 μM SF5. Efficacy of either SF5 (closed circles) or methylene blue formation following zinc acetate capture (open squares) for NaHS was compared by a concentration-response curve (F). $H_2S$ synthesis by P-Gel-derived MΦ lysate was measured by methylene blue formation at 4 h (G) in the presence or absence of L-Cys (10 mM), P5P (2 mM), L-PAG (10 mM), CHH (1 mM). P-Gel-derived MΦ were incubated with and without L-Cys and P5P in living cells with SF5 (1 μM) probe (H). P-Gel-derived MΦ were pre-treated with L-PAG or CHH for 4 h prior and either lysed for methylene blue formation (I) or fluorescent intensity (J) of additional SF5 (1 μM) was assessed over a subsequent 30 min by kinetic assay by spectrofluorometry. ***$P<0.001$, **$P<0.01$, *$P<0.05$ compared by one-way ANOVA and Dunnett's post-test to L-Cys and P5P treated positive controls (n>3).

point is again notable with a sharp peak of resident cells at 0 h that is no longer observed at 4 h, the fluorescence incrementally increases at 24 and 48 h (Fig. 4E).

We applied a similar approach to characterizing a model of air pouch inflammation over 48 h (Fig. 5). Endogenous $H_2S$ formation in the air pouch was monitored using whole mouse fluorescence imaging following injection of the SF5 probe directly into the pouch, 30 min before each sample collection (Fig. 5A). The fluorescent signal within the region of interest (ROI; white dotted line) of the pouch was quantified using Living Image software, with a significant
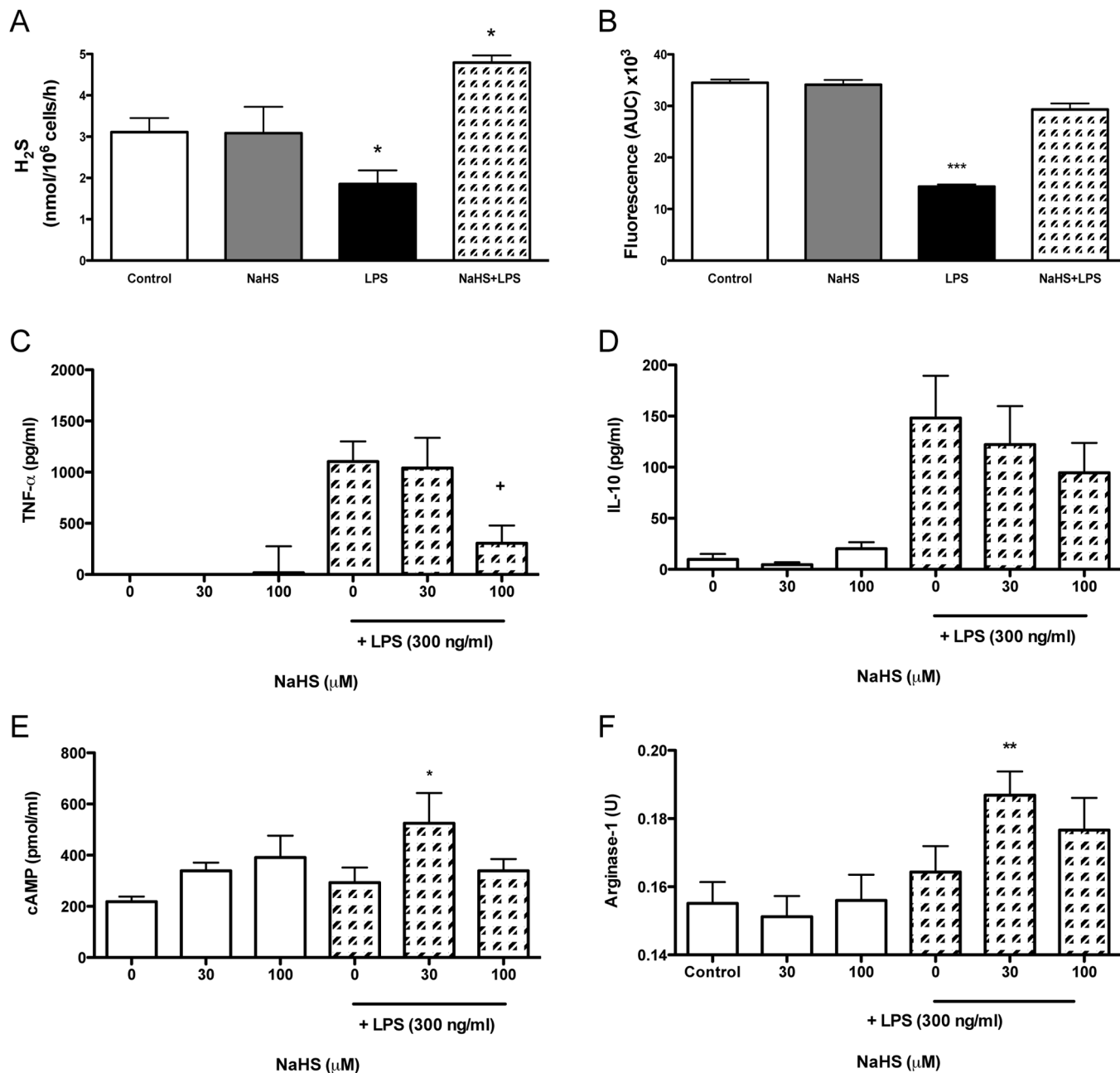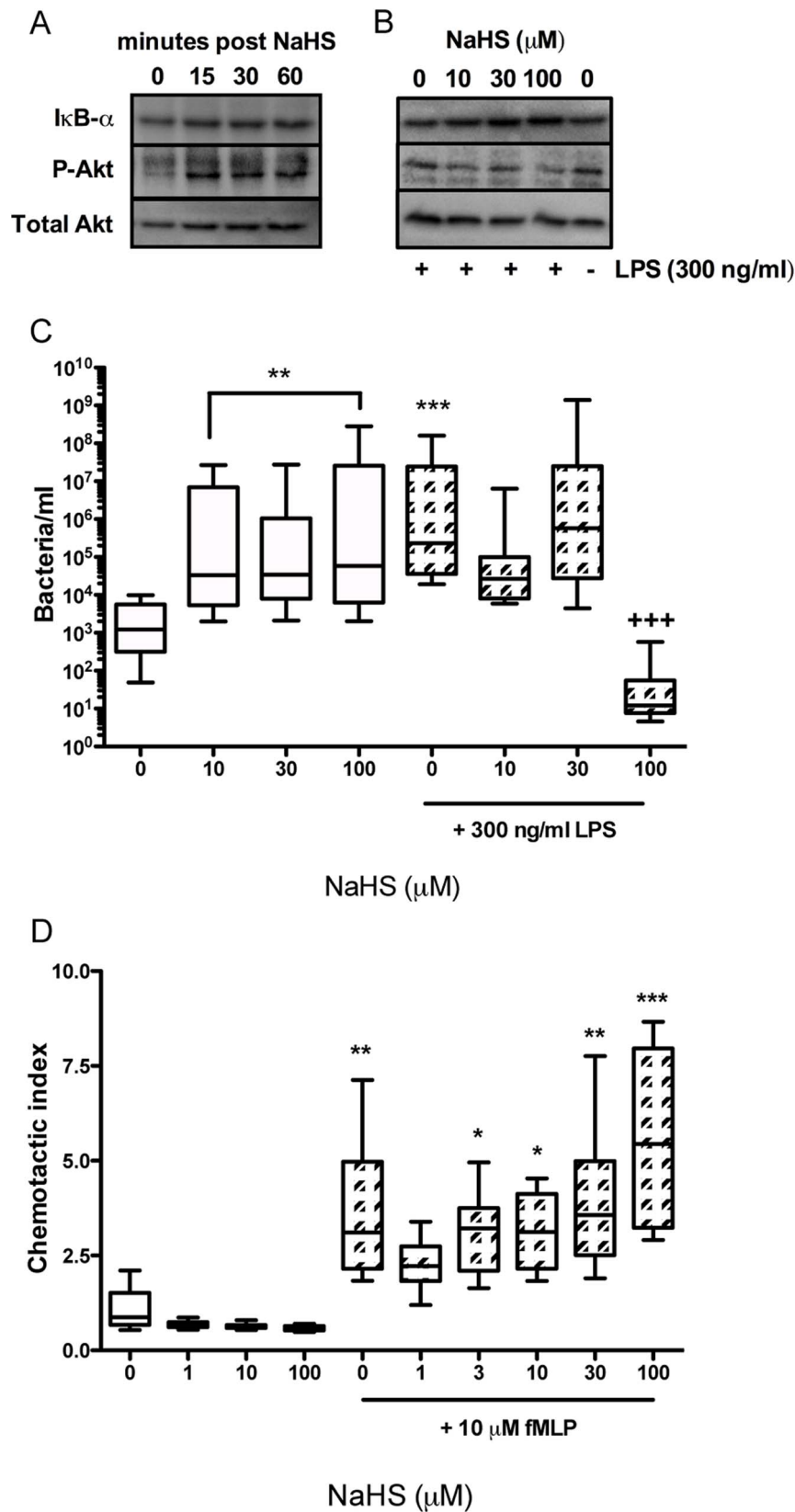
**Figure 2 | Macrophage priming with NaHS reduces classical cell activation.** P-Gel-derived MΦ were treated with NaHS 15 min prior to vehicle or LPS (300 ng/ml; 4 h) and $H_2S$ synthesis was measured by methylene blue formation (A) or SF5 fluorescence (B). The release of cytokines TNF-α (C) and IL-10 (D) were measured in supernatant by ELISA (eBioscience) whereas cAMP levels (E) were measured by EIA (Caymen) and arginase activity (F) were assessed in cell lysate. ***$P<0.001$, **$P<0.01$, *$P<0.05$ compared by one-way ANOVA and Dunnett's post-test to vehicle. (n=5). *$P<0.05$ compared by one-way ANOVA and Dunnett's post-test to vehicle control. +$P<0.05$ as compared by one-way ANOVA and Dunnett's post-test to LPS alone (n=5).

increase ($P<0.01$) in fluorescence at 0 h and 48 h as compared to vehicle (Fig. 5B). As described for peritonitis, the inflammatory exudates were recovered and assessed by spectrofluorometry (Fig. 5C) and flow cytometry (Fig. 4D–I). Note that 0 h is not represented by spectrofluorometry and flow cytometry due to negligible cell numbers that could not be accurately assessed. The histograms and bar graphs are representative of total infiltrating cells (Fig. 5D and G), Gr-1$^{hi}$ (Fig. 4E and H) and F4/80$^+$ (Fig. 4F and I). Each time point is represented by a different colour; 4 h blue, 24 h green and 48 h red with black denoting the isotype control (Fig. 5D–F). SF5 fluorescence intensity within infiltrating leukocytes was significantly increased ($P<0.01$) at 48 h for both total exudate (Fig. 5C) and F4/80$^+$ leukocytes (Fig. 5I) compared to 4 h. SF5 MFI within total and Gr-1$^{hi}$

leukocyte populations was markedly reduced ($P<0.01$) at 24 h (Fig. 5G and H) but increased for F4/80$^+$ leukocytes at 24 and 48 h (Fig. 5I) compared to 4 h.

**Hydrogen sulfide as a marker of neutrophil infiltration and its role in the resolution of inflammation.** Leukocyte infiltrate is used as an indication of acute inflammation. In the early stages of the inflammatory process, neutrophil influx predominates. The decrease in $H_2S$ synthesis that we observed during the first 2–6 h after injection of zymosan into the peritoneum may have been due to inhibitory effects exerted by infiltrating neutrophils. To further examine this, mice were injected i.p. with anti-neutrophil serum (ANS) once at 24 h and again at 1 h prior to injection of zymosan

**Figure 3 | Macrophage priming with NaHS enchances bacterial processing and chemotaxis.** Western blotting for IκB-α and P-Akt was performed on cell lysates treated with NaHS (100 μM) over a time course (A) or in combination with LPS (B). P-Gel-derived MΦ were treated with NaHS 15 min prior to vehicle or LPS (300 ng/ml; 30 min), prior to incubation with ampicillin-resistant *E.coli* for 30 min. P-Gel-derived MΦ were washed and permeabilized and bacterial content recovered. Bacterial growth in LB broth, containing ampicillin, was measured by MTT assay (C) after 24 h and quantified to a standard curve of known bacterial numbers. Chemotactic response of bone marrow derived MΦ was assessed by alamar blue (D) towards 1 μM *f*MLP following 15 min pre-treatment of NaHS. ***P<0.001, **P<0.01, *P<0.05 compared by one-way ANOVA and Dunnett's post-test to untreated control. +++P<0.001 compared by one-way ANOVA and Dunnett's post-test LPS alone (n=5).
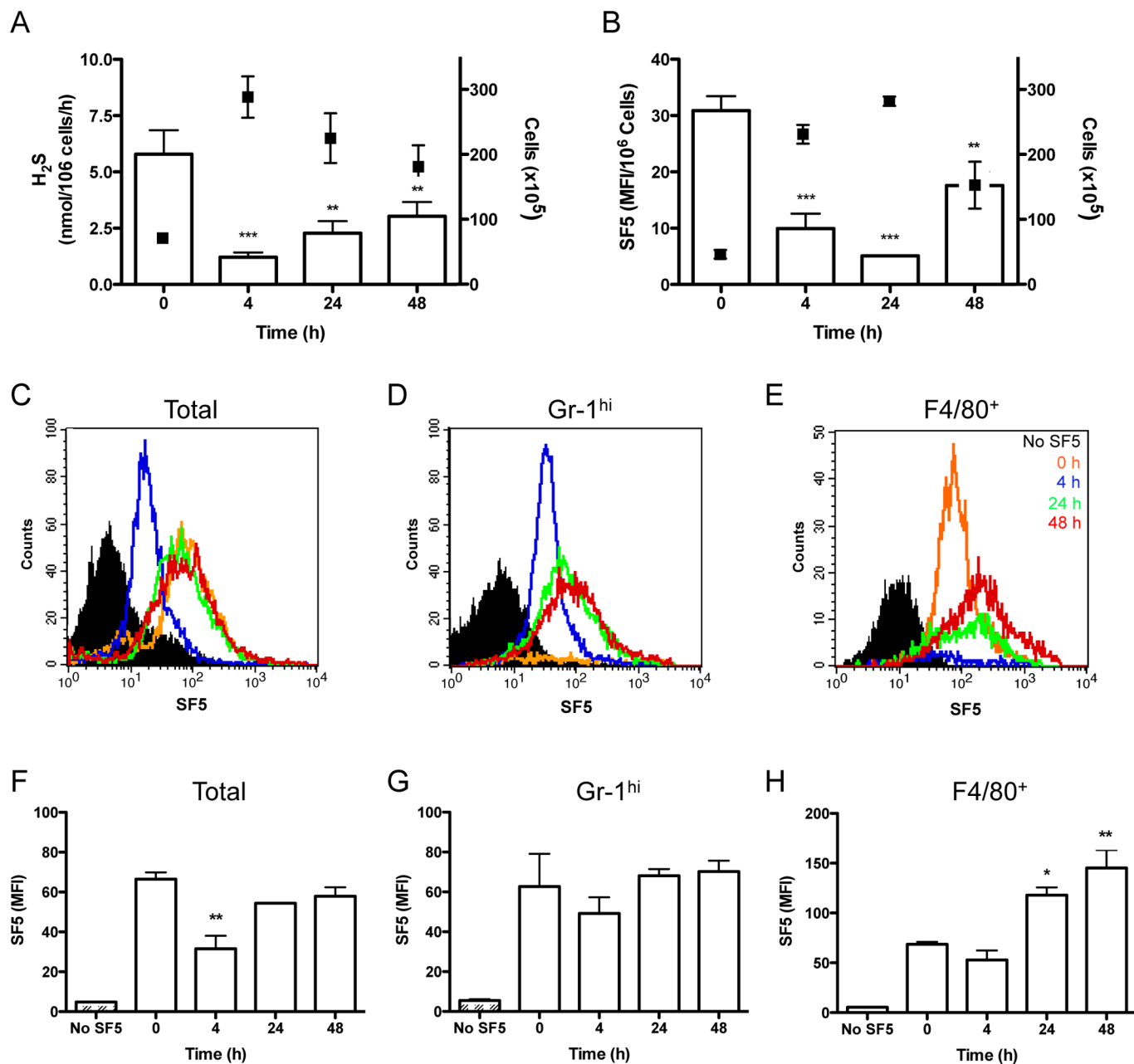
Figure 4 | **Mononuclear cells are an important source of hydrogen sulfide during inflammation: H2S as a mediator of resolution.** The profile of $H_2S$ synthesis by infiltrating leukocytes was compared during zymosan-induced peritonitis measured by methylene blue formation following zinc acetate capture (A) white bars; left Y-axis (n=10) or SF5 probe (B) injected i.p. (100 µl; 10 µM) 30 min prior to euthanasia. SF5 fluorescence intensity was assessed by spectrofluorometry in peritoneal lavage is expressed as a ratio of cell numbers (n>4). Total cell numbers are overlaid (black points; right Y-axis). ***$P<0.001$, **$P<0.01$ compared by one-way ANOVA and Dunnett's post-test to zymosan alone (n>4). SF5 fluorescence within infiltrating leukocytes was analyzed by flow cytometry and represented as histograms over the time course for total infiltrating leukocytes (C) GR-1^{hi} leukocytes (D) and F4/80[+] leukocytes (E). Black filled histograms represents isotype control (C) GR-1 only (D) and F4/80 only (E). Time points are represented as 0 h; orange, 4 h; blue, 24 h; green, and 48 h; red. SF5 mean fluorescence intensity was quantified for total infiltrating leukocytes (F), GR-1^{hi} cells (G) and F4/80^{+} cells (H). **$P<0.01$, *$P<0.05$ compared by one-way ANOVA and Dunnett's post-test to 0 h time point (n>4; representative of 2 experiments).

into the peritoneum (Fig. 6A). The selectivity of ANS for Gr-1^{hi} neutrophils was confirmed by flow cytometry. ANS significantly ($P<0.01$) inhibited the influx of leukocytes into the peritoneal cavity at 4 h (Fig. 6A). This was mirrored by enhanced ($P<0.05$) $H_2S$ synthesis (per $1 \times 10^6$ leukocytes) in ANS-treated mice compared to controls (Fig. 6B).

To investigate whether exogenous or endogenous $H_2S$ was able to affect the acute inflammatory response NaHS, L-PAG or CHH was injected i.p. prior to zymosan-induced peritonitis for 4 h. NaHS treatment, but not cystathionine enzymes inhibition, was able to signifi-

cantly ($P<0.05$) inhibit both total leukocyte and neutrophil infiltration into the peritoneal cavity at 4 h (Fig. 6C and D respectively).

The effect on $H_2S$ production by infiltrating leukocytes of NaHS, L-PAG and CHH pre-treatment was measured by SF5 fluorescence (Fig. 6E) or by flow cytometry (Fig. 6F). Interestingly, only CHH significantly inhibited $H_2S$ synthesis as measured by both methods ($P<0.01$). NaHS reduced $H_2S$ synthesis significantly ($P<0.01$) as measured by flow cytometry (Fig. 6F).

To assess the effects of $H_2S$ later in the inflammatory process, we conducted a series of experiments in both zymosan-induced peri-
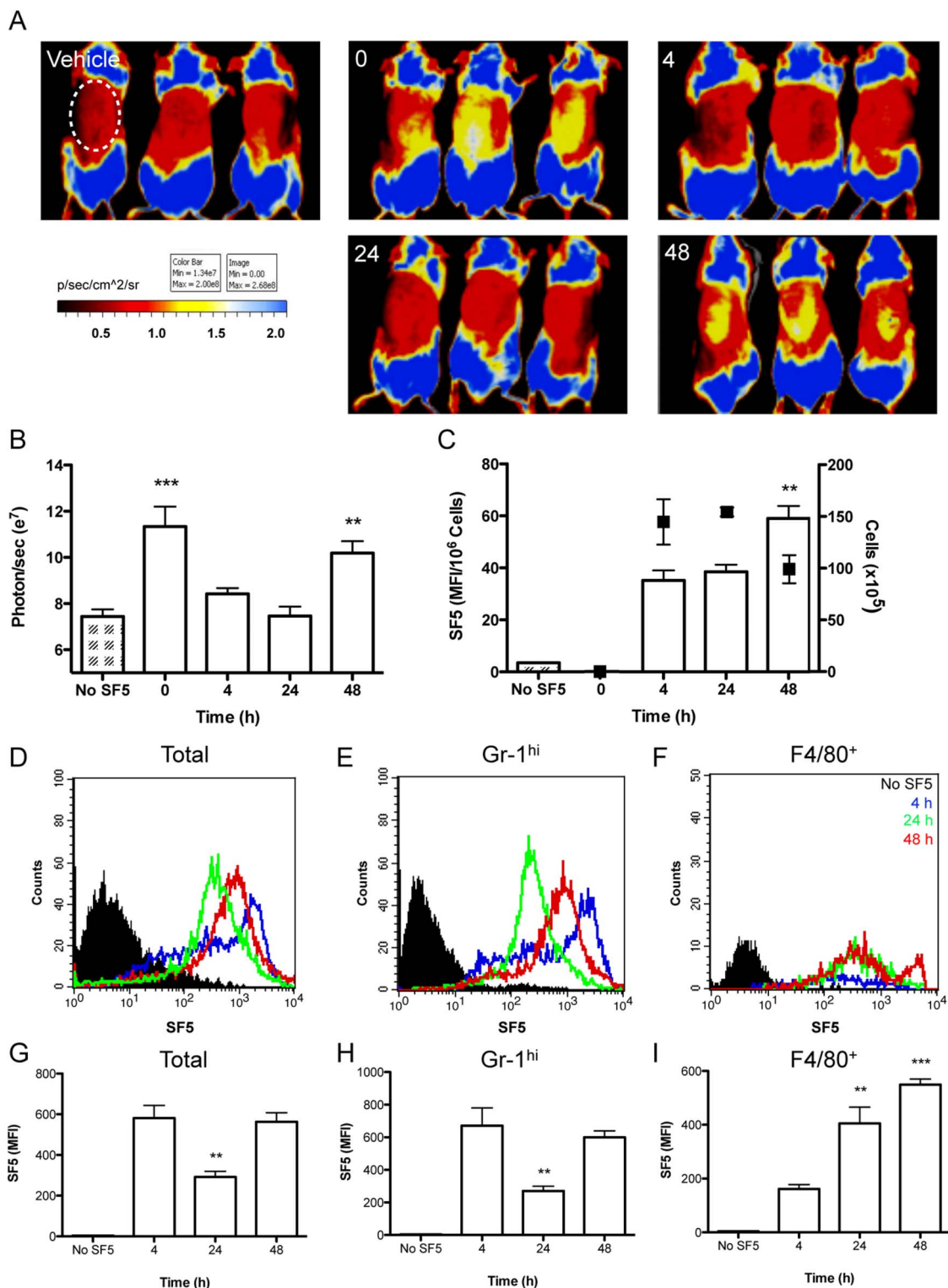
**Figure 5 | Acute inflammation impairs both tissue and cellular hydrogen sulfide synthesis.** Tissue and cellular incorporation of SF5 probe was measured over 48 h in a model of zymosan-induced air pouch inflammation; data are representative of two experiments done in triplicate. Vehicle or SF5 (100 μl; 10 μM) were injected into the pouch 30 min prior to whole mouse imaging with a IVIS Spectrum (Caliper Life Sciences) during a 48 h time course (A). Fluorescence emission was measured within a region of interest (ROI; white dotted line) encapsulating the air pouch expressed as photons/sec over the time course (B). SF5 fluorescence intensity in inflammatory exudates was analyzed by spectrofluorometry (C) and expressed as a ratio of infiltrating cell number (n=3). Total cell numbers are overlaid (black points; right Y-axis). SF5 fluorescence within infiltrating leukocytes was analyzed by flow cytometry and represented as histograms over the time course for total infiltrating leukocytes (E) GR-1$^{hi}$ leukocytes (F) and F4/80$^+$ leukocytes (G). Black filled histograms represents isotype control (E) GR-1 only (F) and F4/80 only (G). Time points are represented as 4 h; blue, 24 h; green, and 48 h; red. SF5 mean fluorescence intensity was quantified for total infiltrating leukocytes (H), GR-1$^{hi}$ (I) and F4/80$^+$ cells (J). **$P<0.01$, *$P<0.05$ compared by one-way ANOVA and Dunnett's post-test compared to 4 h (n=3; representative of 2 experiments).
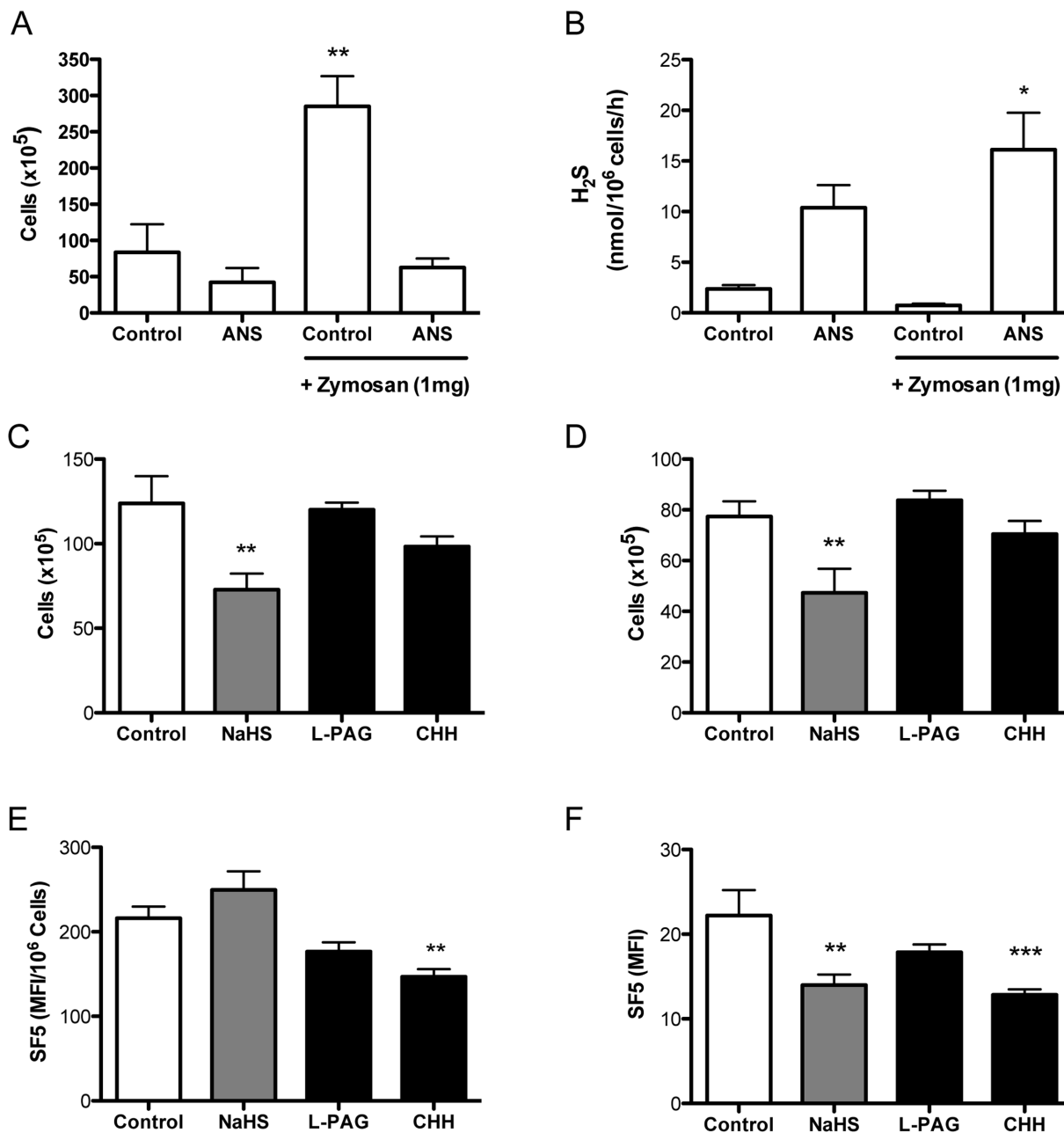
**Figure 6 | Reduction in hydrogen sulfide synthesis during acute inflammation is neutrophil dependent.** Animals received either vehicle or anti-neutrophil serum (ANS) at 24 h and 1 h prior to zymosan-induced peritonitis. Leukocyte numbers were counted by haemocytometer (A) and cell pellets were lysed for methylene blue assay (B). **$P<0.01$, *$P<0.05$ compared by one-way ANOVA and Dunnett's post-test to vehicle alone (n=4). NaHS (-15 min), L-PAG or CHH (1 h) were also injected i.p. prior to zymosan-induced peritonitis for 4 h. Leukocyte numbers were counted by haemocytometer (C) and Gr-1$^{hi}$ neutrophils determined by flow cytometry (D). **$P<0.05$ compared by one-way ANOVA and Dunnett's post-test to zymosan alone (n=5). $H_2S$ synthesis was assessed by SF5 fluorescence intensity using spectrofluorometry in peritoneal lavage and expressed as a ratio of cell numbers (E). Leukocyte SF5 fluorescence was also measured using flow cytometry (F). ***$P<0.001$, **$P<0.01$ compared by one-way ANOVA and Dunnett's post-test to zymosan alone (n=5).

tonitis (Fig. 7A–D) and zymosan-induced air pouch inflammation (Fig. 7E–H). NaHS or CHH were injected i.p 10 h after the initial challenge with zymosan in each model and the samples were collected 48 h after zymosan administration. Leukocyte infiltration was assessed by cell counts (Fig. 7A and E), flow cytometry of Gr-1$^{hi}$ (Fig. 7B and F) and F4/80$^+$ leukocytes (Fig. 7C and G). TNF-α levels were measured in the cell-free exudate (Fig. 7D and H). In both inflammatory models NaHS significantly reduced total leukocyte and neutrophil infiltration, as well as suppressing ($P<0.05$) TNF-α levels in the air pouch exudate. CHH significantly ($P<0.01$) inhibited neutrophil infiltration (Fig. 7B) into the peritoneum, but total leu-

kocyte numbers remained unaffected. The most striking effect was on TNF-α levels. CHH augmented TNF-α levels in both models as compared to controls ($P<0.05$).

## Discussion

This study compares two methods of measuring $H_2S$ synthesis by primary leukocytes and during experimental models of inflammation. We show that primary MΦ expressed both cystathionine enzymes, CSE and CBS, and that they are partially responsible for MΦ $H_2S$ synthesis. Finally, we demonstrate that cystathionine enzyme activity and $H_2S$-induced SF5 fluorescence are negatively regulated, both *in*
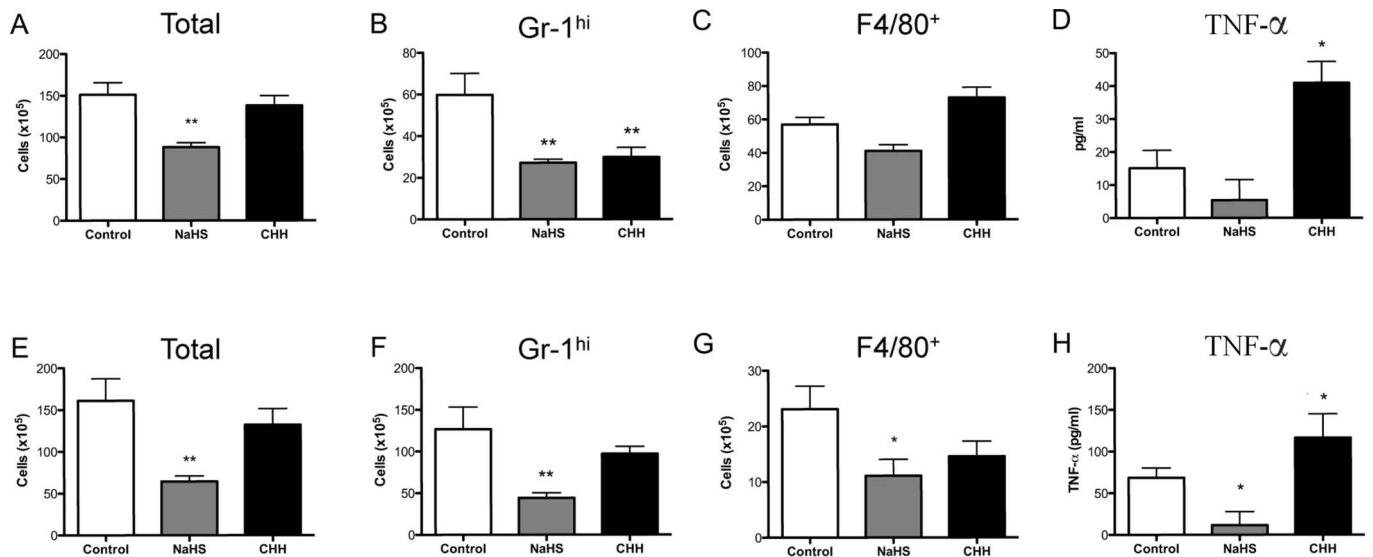
**Figure 7 | Administration of NaHS, but not cystathionine inhibitors, during inflammation enhances leukocyte clearance in zymosan-induced peritonitis and air pouch.** NaHS (5 mg/kg) or CHH (20 mg/kg) were administered i.p. at 10 h after zymosan injection into the peritoneum and total cell infiltrate (A) Gr1^{hi} leukocytes (B) F4/80[+] (C) leukocytes and TNF-α levels (D) where measured at 48 h. **$P<0.01$, *$P<0.05$ compared by one-way ANOVA and Dunnett's post-test to zymosan alone (n>8). NaHS (5 mg/kg) or CHH (20 mg/kg) were administered at 10 h after zymosan injection into the air pouch and total cell infiltrate (E) Gr1^{hi} leukocytes (F) F4/80[+] (G) leukocytes and TNF-α levels (H) where measured at 48 h. **$P<0.01$, *$P<0.05$ compared by one-way ANOVA and Dunnett's post-test to zymosan alone (n>10).

*vitro* and *in vivo,* by inflammatory stimuli. The application of these methodologies revealed the later to be highly sensitive and flexible technique offering applications in both *in vitro* and *in vivo* settings.

Previous studies have reported MΦ $H_2S$ synthesis measured with amperometric microsensor[10] or electrode[8]. We applied a modified method of zinc acetate capture assessed by methylene blue formation using a fluorescence end-point, allowing for greater assay sensitivity. This established technique was compared with a novel fluorescent probe, SF5. The methods differed in a number of important aspects. Firstly, methylene blue formation is a quantifiable method of determining $H_2S$ synthesis over time from tissue/cell lysate. $H_2S$ synthesis via the cystathionine enzymes is dependent on the presence of both L-cysteine and proxidial-5-phosphate as co-factors in this assay, and therefore does not necessary reflect physiological $H_2S$ production. In contrast, sulfidefluor probes are selective markers of intracellular $H_2S$ in live cells without the necessity of additional substrates or co-factors[25]. The SF5 fluorescent signal was visible by immunhisto-chemistry, kinetic assay on a plate reader, by flow cytometry and using an *in vivo* imaging system (IVIS). Despite the multiple applications for SF5, it was not a quantifiable method of measuring $H_2S$ synthesis. Notably, methylene blue formation was more efficient in reacting with $H_2S$ liberated from NaHS in cell-free aqueous solution than SF5 probe. We postulate that in cell-based assays the SF5 probe chelates $H_2S$ within cells over time, rather than reflecting high intracellular concentrations of $H_2S$.

Both methods of monitoring $H_2S$ synthesis were sensitive to pharmacological inhibition of the cystathionine enzymes (CSE and CBS), by L-PAG and CHH, respectively. There was no synergy observed with the combination of both inhibitors, suggesting that $H_2S$ synthesis by these classical pathways accounts for ~50% of the total $H_2S$ synthesis. Recent studies have identified 'alternative' pathways of $H_2S$ synthesis, which may account for the cystathionine-independent signals consistently observed *in vitro*[19,26]. Exposure of MΦ to LPS also resulted in reduced cystathionine enzyme activity and $H_2S$ synthesis, as measured by SF5. Previous studies have reported both positive[10,27] and negative[11,12] regulation of $H_2S$ and CSE expression, with our results being in agreement with the latter. We show that NaHS is protective of endogenous $H_2S$ synthesis as well as priming MΦ to become hyporesponsive to LPS stimulation, regulating both

TNF-α and NO release. These effects could occur via modulation of the NFκB pathways, noted by the lack of IκB-α degradation following NaHS treatment, that has also been observed in other cell types[13,28,29]. NaHS-induced Akt phosphorylation has also been identified as a mechanism of $H_2S$-mediated cell survival[30] and angiogenesis[31]. Akt phosphorylation was differentially regulated in the presence of LPS, which reveals an interesting aspect of the regulatory role of $H_2S$ in the presence or absence of secondary stimuli. The enhanced association, phagocytosis and subsequent processing of *E. coli* observed following treatment with NaHS, as well as a concentration-dependent increase in MΦ migration towards *f*MLP, may point to further signaling pathways involved in membrane reorganization. These processes have also been described in neutrophils with increased survival and anti-bacterial properties[32], as well as modulating neutrophil[33] and endothelial cell[34] migration. These data suggest these are common pathways initiated by NaHS that are shared between different leukocyte populations.

$H_2S$ production is increased in tissue in experimental models of inflammation[5,6] and endotoxic shock[27]. In this study we noted that leukocyte $H_2S$ synthesis was negatively regulated during the acute phases of zymosan-induced inflammation. This response was observed in both zymosan-induced peritonitis and an air-pouch inflammation model at 4–24 h post challenge, when leukocyte infiltrate was at its peak.

During peritonitis, resident cells (~40–60% MΦ) migrate away from the site of challenge to the drain lymph nodes; granulocytes become the predominant leukocyte population 3–6 h post-challenge (~80–90%). By 24 h a mixed population of granulocytes (~60–70%) and monocytes (~20–30%) are the largest constituents within the peritoneum. By 48 h granulocytes become apoptotic and provide an environment in which monocytes can differentiate to mature MΦ (~10–15%)[35]. Interestingly, in our experiments the proportion of MΦ mirrored the capacity of these mixed leukocyte populations to synthesize $H_2S$. Furthermore, the immunodepletion of neutrophils in zymosan-induced peritonitis not only protected, but also enhanced the activity of the cystathionine enzymes in resident leukocytes. A recent study from our laboratory also found that granulocytes were not a prominent source of $H_2S$ production in inflamed colonic tissue[36]. Together these data suggest that MΦ, and not gran-

ulocytes, contribute to the increased levels of $H_2S$ synthesis associated with inflammation. We observed that granulocyte infiltration is associated with reduced $H_2S$ formation under these experimental conditions.

The results obtained from studies using zymosan-induced inflammation of an air-pouch were similar to those from the peritonitis model. Whole animal imaging (IVIS) demonstrated that the greatest $H_2S$ synthesis occurred prior to zymosan-challenge. There are negligible leukocyte populations within the air-pouch prior to challenge, suggesting that the surrounding tissue was synthesizing $H_2S$. This observation would support the well-documented role of $H_2S$ in angiogenesis[31,37] which occurs during the vascularization of the pouch. $H_2S$ has recently been suggested to be a biomarker of disease progression in rheumatoid arthritis[38] and acute lung infection[39]. The present study represents the first description of $H_2S$ measurement in vivo using a non-invasive method, and suggests that this could be translated to the determination of inflammation and leukocyte activation in a clinical setting.

Finally, we assessed whether the addition or inhibition of $H_2S$ during the inflammatory process could significantly affect resolution of inflammation, by monitoring leukocyte clearance and TNF-$\alpha$ levels in vivo. Previous reports suggested that administration of NaHS prior to an inflammatory challenge can result in inhibition of granulocyte infiltration[4]. When NaHS was administered 10 h post-zymosan, a significant reduction of both total cell infiltrate was observed, whereas the CBS inhibitor, CHH, had no effect on total leukocyte infiltration in either the peritonitis or air-pouch models. CHH treatment also resulted in elevated levels of TNF-$\alpha$ within the cell exudates, suggesting a prolongation of the inflammatory response within these animals. Therefore, we suggest that $H_2S$ promotes the phagocytosis and clearance of apoptotic granulocytes by infiltrating mononuclear cells. Taken together with the in vitro studies in primary M$\Phi$, we implicate $H_2S$ as an important homeostatic and pro-resolving mediator in vivo[40].

In conclusion, we provide substantial evidence that $H_2S$ is a potent mediator of leukocyte function both in vitro and in vivo. We observed that acute inflammation, and particularly granulocyte infiltration, significantly inhibits $H_2S$ synthesis. We detail that both the established methylene blue formation assay and a novel sulfidefluor-probe, SF5, can be complimentary methods to measure $H_2S$ synthesis, with the latter providing considerable flexibility for experimental applications. This study highlights the complex relationship between $H_2S$ and inflammatory processes, as well as providing an intriguing proof-of-concept for utilizing fluorescent $H_2S$ probes in vivo.

## Methods

**Antibodies and Reagents.** CHH, LPS and fMLP were obtained from Sigma. Monoclonal anti-human CSE and CBS antibodies were obtained from ABNOVA. Rabbit anti-phospho-Akt and rabbit anti-Pan-Akt or rabbit anti-I$\kappa$B-$\alpha$ obtained from Cell Signaling. Sulfidefluor-5 probe (SF5) was obtained as a kind gift from Dr C. Chang (Berkley, USA). This is a second-generation molecule based upon the structure of published molecules[25].

**Primary cell culture.** P-Gel M$\Phi$ were harvested 4 d after i.p. injection of 1 ml of 2% P-100 gel (Bio-Rad, Ontario, CA) in sterile PBS. Cell suspensions were passed through 40 $\mu$m cell strainers (BD Biosciences, Ontario, CA) before being washed and seeded. Peritoneal cells were harvested as described in 'Zymosan-induced peritonitis and air pouch model'. BMDM$\Phi$ were obtained from femurs and tibias of 22–26 g male Balb/C mice. Bone marrow was flushed, washed and re-suspended in complete DMEM medium containing 30% L929 conditioned medium and incubated at 37°C for 5 days.

Human peripheral blood was collected from healthy volunteers by i.v. withdrawl into 3.2% sodium citrate solution (1:10). PBMCs were separated using Leucosep tubes (Greiner Bio-one, DE) containing Ficoll (GE Healthcare, Ontario, CA). M$\Phi$ were differentiated with 10 ng/ml GM-CSF (Peprotech, New Jersey, USA) for 7 days in complete RPMI media. All healthy volunteers gave oral and written consent, in accordance with McMaster University and Hamilton Health Sciences Research Ethics Boards regulations (11-139-T).

TNF-$\alpha$ and IL-10 secretion measured by ELISA (eBioscience, San Diego, USA). Plates were frozen immediately after treatments (−80°C) for determination of $H_2S$ production and cellular cAMP levels (EIA; Cayman, Michigan, USA).

**Immunohistochemistry.** Cells were cultured on glass slides for fluorescence microscopy. Cells were permeablized with 0.01% Saponin, 0.1% BSA and fixed with 4% PFA. Monoclonal CSE and CBS antibodies (ABNOVA, Taipei City, TW: 1:250) were incubated with the slide overnight prior to 1 h incubation with anti-mouse TRITC (eBioscience, San Diego, CA, USA). Finally slides were mounted with Prolong Gold (Invitrogen, Carlsbad, CA, USA) and images were captured with a Nikon i80 camera. Three fields were analyzed from each donor and representative panels were chosen.

**Hydrogen sulfide synthesis.** Methylene blue formation was performed following zinc acetate capture of $H_2S$ as previously described[5]. This technique was modified from an established assay[41]. Briefly, cells were lysed using ice-cold buffer containing protease inhibitors (Sigma, Ontario, CA). The homogenates were incubated (1.5 h; 37°C) in the presence or absence of P5P (2 mM) and L-Cys (10 mM) unless stated otherwise. Addition of iron (III) chloride and N,N'-dimethyl-p-phenylenediamine sulfate salt (Sigma, Ontario, CA) results in a fluorescent product, read in a 96-well plate with a SpectraMax M3 Microplate reader (Excitation 620 nm, emission 690 nm). Competitive inhibitors of CSE and CBS, L-PAG (10 mM) and CHH (1 mM) respectively, were incubated with M$\Phi$ cultures for 1 h. A standard curve was generated with known concentrations of NaHS.

In vitro SF5 was administered at 1 $\mu$M 30 min prior to performing a 1 h kinetic assay at 37°C with a SpectraMax M3 Microplate reader (Excitation 480 nm, emission 520 nm). In vivo assays were performed by injecting SF5 directly into the site of inflammation 30 min prior to endpoint or imaging.

**Macrophage chemotaxis.** M$\Phi$ chemotaxis was performed using commercially available 5-$\mu$m ChemoTx 96-well plates (Neuroprobe, Maryland, USA). Vehicle, NaHS or fMLP were added to the base of the plate and $10^5$ BMDM$\Phi$ were applied above the membrane. BMDM$\Phi$ were either untreated or pre-treated with NaHS, prior to incubation for 120 min on the membrane. Migrated cells were quantified after 4 h of incubation with alamarBlue (Invitrogen; excitation 540 nm, emission 590 nm) by comparison with a standard curve constructed with known numbers of M$\Phi$.

**Phagocytosis and bacterial killing of *Escherichia coli*.** Ampilcilin-resistant E. coli were generated using a previously described plasmid[42]. P-Gel M$\Phi$ were pre-treated with vehicle, NaHS and/or LPS 30 min prior to exposure to $10^7$ E. coli for 30 min. Cells were washed twice and then permeabilizing with 0.1% saponin (Sigma, Ontario, CA) in lysogeny broth containing ampicillin for 15 min. Supernatants and known concentrations of bacteria were grown for 24 h at 37°C before quantification using tetrazolium salt with absorbance read at 590 nm.

**Western blotting.** Rabbit anti-phospho-Akt (P-Akt), rabbit anti-Pan-Akt or rabbit anti-I$\kappa$B-$\alpha$ (Cell Signaling) were diluted 1:1000 in 5% BSA/TTBS and incubated overnight. HRP-conjugated anti-rabbit antibody (GE Healthcare, ON, Canada) was added 1:5000 dilution and incubated for 1 h. Enhanced chemiluminescence (GE Healthcare, ON, Canada) was captured digitally over 5 min on a Gel Doc XR system and optical density quantified using Image Lab software (BioRad, ON, Canada).

**Zymosan-induced peritonitis and air pouch model.** Peritonitis was induced by injecting 1 mg zymosan A (Sigma, ON, Canada; i.p) in 0.5 ml PBS as previously described[35]. The air pouch procedure was carried out as described previously[43]. Mice were injected with 2.5 ml sterile air intra-dermal (i.d) in the dorsal inter-scapula region with a 23-gauge needle on day 0 and again on day 3 and inflammation was induced by injecting 1% zymosan A in 0.5 ml CMC on day 5. Cells were harvested with PBS-containing 25 U/ml heparin and 0.3 mM EDTA, and counted using trypan blue (Sigma). Proportions of specific leukocyte populations were quantified by flow cytometry staining for granulocytes (GR-1$^{high}$) or myeloid cells (F4/80$^+$). All experimental procedures described herein were approved by the Animal Care Committee of the Faculty of Health Sciences at McMaster University.

**Whole mouse imaging.** Vehicle or SF5 (100 $\mu$l; 10 $\mu$M) were injected into the pouch 30 min prior to whole mouse imaging with an IVIS Spectrum (Caliper Life Sciences) during a 48 h time course. Fluorescence (excitation 460 nm; emission 520) was measured within a region of interest (ROI; white dotted line) encapsulating the air pouch and analyzed using Living Image software.

**Statistical analysis.** All statistics were analyzed on GraphPad Prism 5 software package. One-way ANOVA and Dunnett's post hoc evaluation were applied to grouped data to test the probability of significant differences among treatments. An associated probability ($P$ value) of less than 5% was considered significant.

1. Wallace, J. L. Physiological and pathophysiological roles of hydrogen sulfide in the gastrointestinal tract. *Antioxidants & redox signaling* **12**, 1125–1133 (2010).
2. Wang, R. Hydrogen sulfide: a new EDRF. *Kidney international* **76**, 700–704 (2009).
3. Whiteman, M. a. W., P. Hydrogen sulfide and inflammation: the good, the bad, the ugly and the promising. *Expert Review of Clinical Pharmacology* **4**, 13–32 (2011).
4. Zanardo, R. C. et al. Hydrogen sulfide is an endogenous modulator of leukocyte-mediated inflammation. *Faseb J* **20**, 2118–2120 (2006).

5.  Wallace, J. L., Vong, L., McKnight, W., Dicay, M. & Martin, G. R. Endogenous and exogenous hydrogen sulfide promotes resolution of colitis in rats. *Gastroenterology* **137**, 569–578, 578 e561 (2009).

6.  Wallace, J. L., Dicay, M., McKnight, W. & Martin, G. R. Hydrogen sulfide enhances ulcer healing in rats. *Faseb J* **21**, 4070–4076 (2007).

7.  Linden, D. R. *et al.* Production of the gaseous signal molecule hydrogen sulfide in mouse tissues. *Journal of neurochemistry* **106**, 1577–1585 (2008).

8.  Whiteman, M. *et al.* The effect of hydrogen sulfide donors on lipopolysaccharide-induced formation of inflammatory mediators in macrophages. *Antioxidants & redox signaling* **12**, 1147–1154 (2010).

9.  Zhi, L., Ang, A. D., Zhang, H., Moore, P. K. & Bhatia, M. Hydrogen sulfide induces the synthesis of proinflammatory cytokines in human monocyte cell line U937 via the ERK-NF-kappaB pathway. *Journal of leukocyte biology* **81**, 1322–1332 (2007).

10. Zhu, X. Y., Liu, S. J., Liu, Y. J., Wang, S. & Ni, X. Glucocorticoids suppress cystathionine gamma-lyase expression and H2S production in lipopolysaccharide-treated macrophages. *Cell Mol Life Sci* **67**, 1119–1132 (2010).

11. Lee, M., Sparatore, A., Del Soldato, P., McGeer, E. & McGeer, P. L. Hydrogen sulfide-releasing NSAIDs attenuate neuroinflammation induced by microglial and astrocytic activation. *Glia* **58**, 103–113 (2010).

12. Hu, L. F., Wong, P. T., Moore, P. K. & Bian, J. S. Hydrogen sulfide attenuates lipopolysaccharide-induced inflammation by inhibition of p38 mitogen-activated protein kinase in microglia. *Journal of neurochemistry* **100**, 1121–1128 (2007).

13. Oh, G. S. *et al.* Hydrogen sulfide inhibits nitric oxide production and nuclear factor-kappaB via heme oxygenase-1 expression in RAW264.7 macrophages stimulated with lipopolysaccharide. *Free radical biology & medicine* **41**, 106–119 (2006).

14. Maclean, K. N. *et al.* Cystathionine beta-synthase null homocystinuric mice fail to exhibit altered hemostasis or lowering of plasma homocysteine in response to betaine treatment. *Molecular genetics and metabolism* **101**, 163–171 (2010).

15. Ishii, I. *et al.* Cystathionine gamma-Lyase-deficient mice require dietary cysteine to protect against acute lethal myopathy and oxidative injury. *The Journal of biological chemistry* **285**, 26358–26368 (2010).

16. Hirata, I. *et al.* Endogenous hydrogen sulfide is an anti-inflammatory molecule in dextran sodium sulfate-induced colitis in mice. *Digestive diseases and sciences* **56**, 1379–1386 (2011).

17. Zhang, H., Moochhala, S. M. & Bhatia, M. Endogenous hydrogen sulfide regulates inflammatory response by activating the ERK pathway in polymicrobial sepsis. *J Immunol* **181**, 4320-4331 (2008).

18. Bhatia, M. *et al.* Role of hydrogen sulfide in acute pancreatitis and associated lung injury. *Faseb J* **19**, 623–625 (2005).

19. Shibuya, N., Mikami, Y., Kimura, Y., Nagahara, N. & Kimura, H. Vascular endothelium expresses 3-mercaptopyruvate sulfurtransferase and produces hydrogen sulfide. *Journal of biochemistry* **146**, 623–626 (2009).

20. Shen, X. *et al.* Measurement of plasma hydrogen sulfide in vivo and in vitro. *Free radical biology & medicine* **50**, 1021–1031 (2011).

21. DeLeon, E. R., Stoy, G. F. & Olson, K. R. Passive loss of hydrogen sulfide in biological experiments. *Analytical biochemistry* **421**, 203–207 (2011).

22. Shatalin, K., Shatalina, E., Mironov, A. & Nudler, E. H2S: a universal defense against antibiotics in bacteria. *Science (New York, N.Y* **334**, 986–990 (2011).

23. Sasakura, K. *et al.* Development of a highly selective fluorescence probe for hydrogen sulfide. *Journal of the American Chemical Society* **133**, 18003–18005 (2011).

24. Peng, H. *et al.* A fluorescent probe for fast and quantitative detection of hydrogen sulfide in blood. *Angewandte Chemie International ed* **50**, 9672–9675 (2011).

25. Lippert, A. R., New, E. J. & Chang, C. J. Reaction-based fluorescent probes for selective imaging of hydrogen sulfide in living cells. *Journal of the American Chemical Society* **133**, 10078–10080 (2011).

26. Mikami, Y. *et al.* Thioredoxin and dihydrolipoic acid are required for 3-mercaptopyruvate sulfurtransferase to produce hydrogen sulfide. *The Biochemical journal* **439**, 479–485 (2011).

27. Li, L. *et al.* Hydrogen sulfide is a novel mediator of lipopolysaccharide-induced inflammation in the mouse. *Faseb J* **19**, 1196–1198 (2005).

28. Chattopadhyay, M. *et al.* Hydrogen sulfide-releasing aspirin suppresses NF-kappaB signaling in estrogen receptor negative breast cancer cells in vitro and in vivo. *Biochemical pharmacology* **83**, 723–732 (2011).

29. Pan, L. L., Liu, X. H., Gong, Q. H. & Zhu, Y. Z. S-Propargyl-cysteine (SPRC) attenuated lipopolysaccharide-induced inflammatory response in H9c2 cells involved in a hydrogen sulfide-dependent mechanism. *Amino acids* **41**, 205–215 (2011).

30. Shao, J. L. *et al.* H2S protects hippocampal neurons from anoxia-reoxygenation through cAMP-mediated PI3K/Akt/p70S6K cell-survival signaling pathways. *J Mol Neurosci* **43**, 453–460 (2011).

31. Cai, W. J. *et al.* The novel proangiogenic effect of hydrogen sulfide is dependent on Akt phosphorylation. *Cardiovascular research* **76**, 29–40 (2007).

32. Rinaldi, L. *et al.* Hydrogen sulfide prevents apoptosis of human PMN via inhibition of p38 and caspase 3. *Laboratory investigation; a journal of technical methods and pathology* **86**, 391–397 (2006).

33. Dal-Secco, D. *et al.* Hydrogen sulfide augments neutrophil migration through enhancement of adhesion molecule expression and prevention of CXCR2 internalization: role of ATP-sensitive potassium channels. *J Immunol* **181**, 4287–4298 (2008).

34. Pupo, E. *et al.* Hydrogen sulfide promotes calcium signals and migration in tumor-derived endothelial cells. *Free radical biology & medicine* **51**, 1765–1773 (2011).

35. Damazo, A. S., Yona, S., Flower, R. J., Perretti, M. & Oliani, S. M. Spatial and temporal profiles for anti-inflammatory gene expression in leukocytes during a resolving model of peritonitis. *J Immunol* **176**, 4410–4418 (2006).

36. Flannigan, K. L., McCoy, K. D. & Wallace, J. L. Eukaryotic and Prokaryotic Contributions to Colonic Hydrogen Sulfide Synthesis. *American journal of physiology* **301**, 188–193 (2011).

37. Wang, M. J. *et al.* The hydrogen sulfide donor NaHS promotes angiogenesis in a rat model of hind limb ischemia. *Antioxidants & redox signaling* **12**, 1065–1077 (2011).

38. Whiteman, M. *et al.* Detection of hydrogen sulfide in plasma and knee-joint synovial fluid from rheumatoid arthritis patients: relation to clinical and laboratory measures of inflammation. *Annals of the New York Academy of Sciences* **1203**, 146–150 (2011).

39. Chen, Y. H. *et al.* Serum hydrogen sulfide as a novel marker predicting bacterial involvement in patients with community-acquired lower respiratory tract infections. *Respirology (Carlton, Vic* **14**, 746–752 (2009).

40. Wallace, J. L., Ferraz, J. G. & Muscara, M. N. Hydrogen Sulfide: An Endogenous Mediator of Resolution of Inflammation and Injury. *Antioxidants & redox signaling* (2012).

41. Stipanuk, M. H. & Beck, P. W. Characterization of the enzymic capacity for cysteine desulphhydration in liver and kidney of the rat. *The Biochemical journal* **206**, 267–277 (1982).

42. Hapfelmeier, S. *et al.* The Salmonella pathogenicity island (SPI)-2 and SPI-1 type III secretion systems allow Salmonella serovar typhimurium to trigger colitis via MyD88-dependent and MyD88-independent mechanisms. *J Immunol* **174**, 1675–1685 (2005).

43. Perretti, M., Harris, J. G. & Flower, R. J. A role for endogenous histamine in interleukin-8-induced neutrophil infiltration into mouse air-pouch: investigation of the modulatory action of systemic and local dexamethasone. *British journal of pharmacology* **112**, 801–808 (1994).

## Acknowledgements

## Author contribution

All experiments were conducted at McMaster University by N.D. under the supervision of J.W. N.D. and J.W. designed experiments; N.D. and J.N. performed research; N.D. analyzed data; N.D., E.V. and J.W. prepared the manuscript.

## Additional information

Dr C. Chang, of the University of California, Berkley, gave permission for the use of the SF5 molecule in this study.